Studia Quaternaria, vol. 41, no. 2 (2024): 43–53 DOI: 10.24425/sq.2024.149971

THE ÁRPÁD MOUND – GEOARCHEOLOGICAL RESEARCH OF A BURIAL MOUND IN THE CENTRAL CARPATHIAN BASIN

Péter Cseh[1], Dávid Molnár[1], László Makó[2], Pál Sümegi[1]

[1] *Department of Geology and Paleontology, University of Szeged, H-6722 Szeged, Egyetem u. 2-6, Hungary; e-mail: cspeter@geo.u-szeged.hu, molnard@geo.u-szeged.hu, sumegi@geo.u-szeged.hu*

[2] *Faculty of Agriculture, Institute of Plant Sciences and Environmental Protection, University of Szeged, H-6722 Szeged, Egyetem u. 2-6, Hungary; e-mail: makol@geo.u-szeged.hu*

** corresponding author*

Abstract:
Kurgans hold exceptional archaeological, natural, and environmental historical significance in the lowland landscape of Eastern Europe, which has been extensively altered by millennia of agricultural activity. By conducting comparative soil and sedimentological analyses of the buried soil levels from kurgan construction, as well as the recent surface soil, we can uncover environmental changes from the latter half of the Holocene. These analyses also reveal how prehistoric human activities influenced local soil and environmental conditions. Our research focused on a geoarchaeological examination of a burial mound in the Hungarian Great Plain. Sedimentological analyses, including grain size distribution and magnetic susceptibility measurements, were performed on samples extracted by drilling from this mound. This comprehensive investigation enabled us to distinguish between different construction layers in the kurgan's soil material and compare them. Additionally, it was possible to reconstruct steppe-like environmental conditions in the local surroundings of the kurgan before and during its construction.

Key words: magnetic susceptibility, geoarchaeology, sedimentology, kurgan, Yamnaya.

Manuscript received 16 August 2024, accepted 15 October 2024

INTRODUCTION

The examination of archaeological monuments has become a crucial aspect in reconstructing the former Holocene environment, alongside natural sedimentary basins. These artifacts include former settlement sites such as tells, hillforts, shell mounds, and burial mounds, referred to as kurgans in the Eastern European steppes (Sümegi *et al.*, 2015). Such research can be linked to investigating and determining the timeline of landscape evolution (Derese *et al.*, 2010; Kinnaird *et al.*, 2013) and, ultimately, examining the relationship between humans and their environment during the Holocene (Zhen, 2021).

Lowland landscapes of Hungary and Eastern Europe are dotted with kurgans, most of which can be dated back to the Late Copper to Early Bronze Age (3300–2500 BC). These mounds are associated with the Yamnaya culture, known for their pit-grave kurgans and widespread presence in Eastern Europe and Western Asia (Dani and Horváth, 2012). In Hungary, which is the westernmost widespread area the Yamnaya, these stockbreeding nomads built such mounds for funerary purposes and can typically be found on elevated areas near river banks (Ecsedy, 1979; Dani and Horváth, 2012).

Kurgans were made up of multiple layers of different soils and sediment strata, which can be examined (Bede *et al.*, 2015; Cseh *et al.*, 2022). They were erected on the existing ground surface, where the first burial was placed, and the surrounding earth was utilized as construction material (Barczi *et al.*, 2003; Barczi, 2004; Joó *et al.*, 2007). These processes altered the soil of the mounds, resulting in disturbed anthropogenic soils with characteristics of the original soil, while the previously buried soil horizon remains undisturbed. The alterations in this modified soil can be identified and compared to the undisturbed buried soil profile (Cseh *et al.*, 2022).

The investigation of burial mounds in Hungary started during the 19th century, initially specifically for archaeological, botanical, or cadastral purposes (Rómer, 1878). In the 20th century, geological and pedological methods were introduced to describe the stratigraphy of these monuments. Currently, the study of these mounds extends beyond the boundaries of traditional archaeology. The examination of soil, sedimentary properties, and the refinement of these approaches enable the reconstruction of the changing environmental factors throughout the history of the Holocene. Kurgans are significant because the continuous changes in soil, ecological, and climatic conditions make it rare for soil properties from past environments to remain intact. Therefore, it is necessary to find specific places, like kurgans, where conditions allowed for the retention of these properties. In these monuments, the buried soil layers beneath the kurgans, influenced by human activity, have maintained the characteristics of the earlier environment (Alexandrovskiy, 1996). Recent geoarchaeological surveys have provided a path for paleoenvironmental reconstructions, thereby enabling researchers to gauge the intensity of soil formation processes over the past 5000 years (Alexandrovskiy, 2000; Zaitseva *et al.*, 2005; Demkin *et al.*, 2008).

The large number of kurgans in Hungary and Eastern Europe has provided opportunities for a wide range of investigative methods and approaches. A comprehensive summary of these can be found in the 2011 volume by Pető and Barczi (2011), which consolidates recent kurgan research in the region. These mounds are not only associated with a specific period but have also been observed in both the Pit-Grave and Timber-Grave cultures. The investigative methods include archaeological, anthropological, pedological, paleopedological, geochemical, and botanical (both paleo and recent) approaches (Pető and Barczi, 2011).

STUDY AREA

The Árpád Mound, situated at coordinates N 46°33'25", E 19°58'06", is located in the central region of the Carpathian Basin (Fig. 1A). It occupies a region within the Danube-Tisza interfluve of the Great Hungarian Plain. The elevation of the site is 88 m, and the mound itself rises 6 m above the average elevation of the surrounding plain, which is approximately 82 m. Its diameter is approximately 35 m, with a 12-m limestone obelisk at its center, built at the end of the 19th century (Fig. 1C, D).

The geological development history of the area is predominantly characterized by the accumulation and transportation of river and wind-borne sediments. During the late Pleistocene, a notable amount of alluvial Quaternary sandy sediments was deposited in the area as the previous alluvium of the Danube River flowed through it. At the end of the Pleistocene, these sediments were sorted into sand dunes through eolian activity (Sümegi, 2002). Additionally, the loessy areas of the Danube-Tisza region are a consequence of dust fall during the late Pleistocene. During the Holocene, river-related floodplain sediments became significant in areas near the Tisza (Fig. 1B) (Molnár, 2015). Based on the most comprehensive and up-to-date study

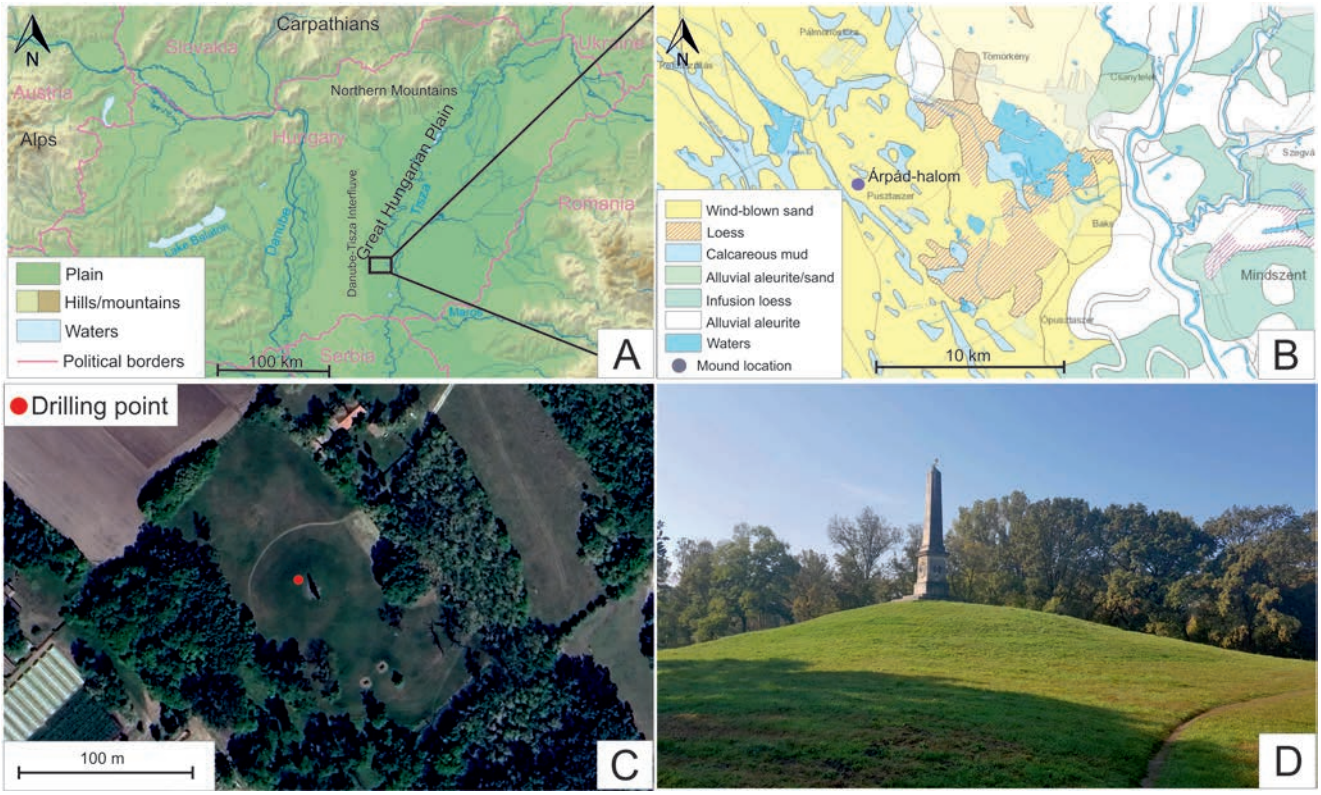

Fig. 1. A, Location of the Árpád Mound in Hungary (Wikimedia Commons); B, Surface geological map of the vicinity of the study area (Gyalog and Síkhegyi, 2005); C, Satellite image of the mound the surrounding areas (Google Earth); D, Árpád Mound (from the North) – made by the authors.

by Lehmkuhl *et al.* (2021) covering the entire Quaternary loess and loess-like sediments of Europe, these European aeolian sediments can be divided into 6 major domains and 17 subdomains. Their formation is influenced by various geomorphological and paleoenvironmental factors, such as river transport, ice sheet fluctuations, permafrost boundaries, and vegetation cover, resulting in diverse depositional characteristics across Europe. The studied area falls within domain IV, the Middle Danube Basin loess region, characterized by sandy loess and, in the former floodplain of the Tisza River, covered by alluvial and fluvial deposits. These findings strongly support the results of previous research.

These geological and the climatic conditions have resulted in well-characterized soil conditions in this area. Significant meadow and alluvial soils have developed in the Tisza alluvium. Sandy areas are characterized by sandy soils and humic sandy soils, while areas with loessy or loessy-sandy parent material are characterized by sandy soils of the chernozem type. In areas with lower elevation, higher groundwater levels support the appearance of meadow chernozems (Stefanovits, 1972; Lehmkuhl *et al.*, 2021).

Since the Pleistocene, the Carpathian Basin has exhibited a mosaic environment in terms of plant cover. Today, the lowland region of Hungary can be considered as the part of the Eurasian forest-steppe belt, which includes steppe meadows, steppe scrub, and a mosaic of oak forests (Sümegi *et al.*, 2012; Cseh *et al.*, 2022).

The area of Hungary, including the region between the Danube and Tisza rivers (Fig. 1A), is situated within the temperate climate zone. The Carpathian Basin is affected by three main climatic influences: the western oceanic, the southern Mediterranean, and the northeastern dry continental. According to the Holdridge classification system, which is based on the potential evapotranspiration rate, mean annual precipitation, and mean annual temperature, this region is classified as a cold temperate grassland (Holdridge, 1947). The Péczely classification system categorizes it as warm and dry region (Péczely, 1979). The mean temperature in the eastern part of the southern Great Plain is approximately 10.5°C, with July being the warmest month (average temperature of 21.8°C) and January being the coldest month (average temperature of 1°C). The average annual precipitation is quite low, ranging from 500 to 550 mm, with 300–350 mm falling during the growing season, making it one of the driest regions in the country.

MATERIAL AND METHODS

Sampling and Macroscopic Analysis

In order to obtain an ample amount of material for the various measurements, a motorized spiral drill with a 4 cm diameter was utilized to execute the sampling procedure. The external part of the samples was extracted to avert contamination due to the exposed auger and was not incorporated in the subsequent evaluation of the sediments. The samples were extracted with continuous, undisturbed sampling, with the interval of 5 cm. As a result, the section of 377 cm yielded a collection of 74 samples for further analysis.

The sediment and soil layers were analyzed utilizing general stratigraphic principles at the research site. The wet color of the samples was assessed with the Munsell Color Chart (Munsell, 2000), establishing a dependable foundation for further differentiation of sediment and soil layers. This standardized process provides the opportunity to compare the continuous sediment material of this kurgan with data sets obtained from other, even fully excavated mounds. Identification of soil layers was performed in accordance with the Hungarian Soil Classification System (Stefanovits, 1972), which enables precise differentiation of various subtypes of Chernozem soils. The WRB classification (IUSS Working Group, 2015; Michéli *et al.*, 2019) can be cross-referenced with this system. Classic chernozem soil can be classified as chernozem, while meadow (hydromorphic) chernozem is classified as gleysols. As a result, meadow chernozem is a more accurate description of a chernozem-like soil impacted by fluctuating groundwater, from a soil genetic perspective.

Gran Size Analysis

The determination of the grain-size composition followed the Bokhorst's principles (Bokhorst, 2011). Prior to the measurements, samples underwent pre-treatment using hydrogen peroxide (30% H_2O_2) and hydrochloric acid (10% HCl) to eliminate organic material and carbonates. Subsequently, 0.7 g of the sample was mixed with 30 mL of sodium hexametaphosphate (Na_2P6O_{18}) solution to disaggregate individual granules. Samples were also subjected to ultrasonic cleaning to prevent disaggregation of the grains. The prepared suspensions were then filtered through a 0.5 mm sieve. Subsequently, the grain-size composition was analyzed using an Easysizer 20 laser sedigraph instrument at the Department of Geology and Paleontology, the University of Szeged. This instrument uses 2 MW of energy and a He-Ne laser with 0.6328 μm wavelength (Sümegi *et al.*, 2019) and it measures 42 particle size ranges between 0.0001 and 0.5 mm with its 54 built-in detectors. The results were presented in line diagrams, with particle size ranges classified based on the Wentworth scale (Wentworth, 1922).

Magnetic Susceptibility

Magnetic susceptibility is a parameter that quantifies the content of magnetizable elements in sediments. To measure this parameter, bulk samples were prepared and homogenized using a porcelain mortar prior to analysis. Measurements were performed on every sample (the interval of 5 cm) using a Bartington MS2 Magnetic Susceptibility Meter operating at a frequency of 2.7 MHz (Dearing, 1999). Three replicate measurements were taken from each sample

and the mean value was calculated. The magnetic susceptibility values reported in this study are presented in units of $\times 10^{-8} m^3 kg^{-1}$ SI.

Organic Matter and Carbonate Content Analysis

In order to evaluate the proportion of organic matter and carbonate content in the samples, Dean's Loss on Ignition method was applied (Dean, 1974; Hieri *et al.*, 2001). This method is commonly utilized for quantifying the carbonate and organic matter content in carbonaceous sediments. Initially, the 74 samples were air-dried for 24 hours at 65°C and then homogenized in a porcelain mortar. The weight of the crucibles used was determined to the nearest 0.0001 g (m_c), and approximately 3 g of the sample was added. The crucibles were then subjected to heating at 105°C (for 24 hours) and weighed (m_{105}). After further heating at 550°C (for 2.5 hours), the crucibles were weighed again (m_{550}). The organic matter content was subsequently computed, and further heating at 900°C (for 2.5 hours) was performed on the same samples to calculate the carbonate content using the following formulae:

$$\text{Organic matter content (\%)} = 100 - ((m_{550} - m_c)/(m_{105} - m_c)) \times 100$$

$$\text{Carbonate content (\%)} = 100 - ((m_{900} - m_c)/(m_{550} - m_c)) \times 100$$

The quantified percentages of organic matter and carbonate within sediment samples are representative of their Total Organic Carbon (TOC) and Total Inorganic Carbon (TIC) contents, respectively.

Radiocarbon Measurement

The Nuclear Research Center of the Hungarian Academy of Sciences in Debrecen (Hungary) conducted AMS ^{14}C radiocarbon dating on a charcoal fragment sample discovered in the burial level of the mound. The preparation of the sample and the measurement followed the procedures described by Hertelendi *et al.* (1989) and Molnár *et al.* (2013). To determine the calendar and BP ages, the conventional radiocarbon ages were calibrated using IntCal 20 calibration curves (Reimer *et al.*, 2020) and presented with a 2-sigma confidence level (>95% for each sample) by using the CALIB 8.1.0 software.

RESULTS

Results of Macroscopic Layer Description

Through the macroscopic examination of the section drilled at the central part of the kurgan, the general construction layers could already be distinguished based on the Munsell Color Chart, i.e. color of the layers, the material of the soil, and the state of its compaction (Fig. 2).

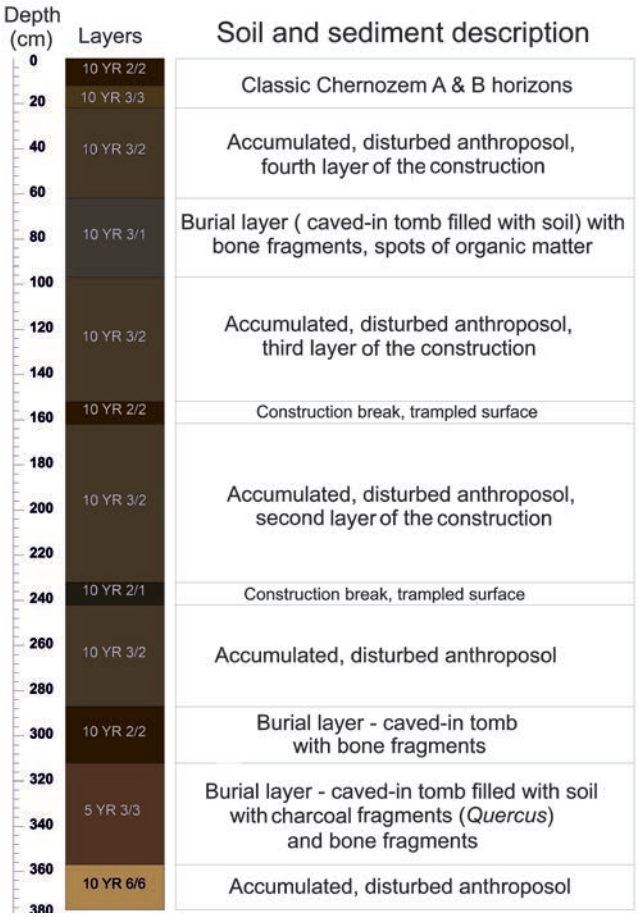

Fig. 2. The different layers of the drilling section of the mound with short macroscopic descriptions. The codes found in the stratigraphic sequence represent the Munsell colors of the respective layers, with the coloring of the layers corresponding accordingly.

The sedimentary layer below 377 cm constitutes the bedrock of the kurgan's parent material and consists of yellowish-grey wind-blown sand with some carbonate. This sediment can be observed in the surroundings of the examined area in the form of oval hills and elongated residual ridges. Between 357 cm and 377 cm, a reddish-brown (10YR 3/6) fine sand/very fine sand layer can be found with burnt traces in the sediment material.

Above this layer, between 312 cm and 357 cm, a layer with a color of 5YR 3/3 (dark reddish brown) can be found. Based on its structure, it could have been a burial chamber filled with soil, which is also evident macroscopically by the presence of charred wood remains.

Above it, between 287 cm and 312 cm, another layer filled with soil associated with a presumed collapsed burial chamber can be observed, with soil material of a color 10YR 2/2 (very dark brown). Organic matter spots and small bone remains can also be found in its material.

Subsequently, the material of the first construction layer of the kurgan can be found between 287–232 cm. It can be divided into two parts. The lower part (between

242–287 cm) is a soil material rich in charcoal with a color of 10YR 3/2 (very dark grayish brown), on the top of which a compacted layer of 10 cm can be found with a color of 10YR 2/1 (black) (between 232–242 cm). This 10 cm can be distinguished as the upper part of this construction layer.

On the top of the previous layer, the second construction layer of the kurgan (between 232–162 cm) was deposited. This level can also be divided into two parts. The lower part between 232–162 cm is a disturbed blackish-brown (10YR 3/2) soil layer. The upper 10 cm of this layer (between 152 cm and 162 cm) can be described as a compacted layer again with a color of 10YR 2/2 (very dark brown).

Between 152–62 cm, the third construction layer can be found with a thickness of almost 1 meter. The lower part of this layer between 152–97 cm is a disturbed blackish-brown (10YR 3/2) soil. Within this layer (between 62–97 cm), another – presumably collapsed – disturbed zone can be observed with organic matter spots, small snail shells and bone fragments. On top of this, between 97 cm and 62 cm, a thicker layer of blackish-brown (10YR 3/2) soil can be found which can be interpreted as the fourth construction layer.

The uppermost level of the kurgan is the recent soil, which, based on its macroscopic characteristics, can be considered as the A (0–12 cm, color: 10YR 2/2) and B (12–22 cm, color: 10YR 3/3) horizons of chernozem soil.

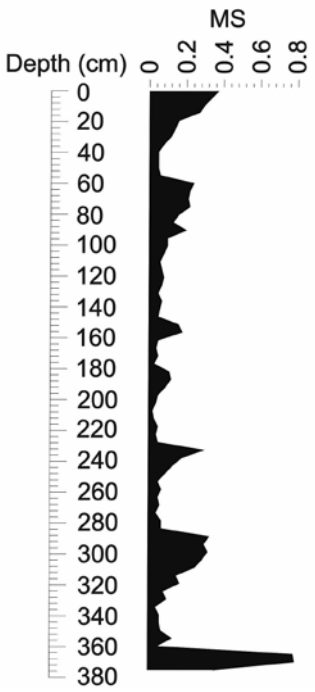

Fig. 3. The results of magnetic susceptibility (MS) measurements conducted on samples extracted from the drill core of the Árpád Mound.

Magnetic susceptibility results

The magnetic susceptibility results measured in the drill core section show a highly varied picture in terms of the magnetic element content of the section, allowing for the identification and delineation of distinct layers (Fig. 3).

The maximum value of MS in the section was found in the lowest layer (357–377 cm), where it reaches a value of 0.8 between 362–372 cm. This could indicate the presence of iron-rich ochre used in burial practices (Ecsedy, 1979), which contains significant proportion of iron, thus can cause high MS values, but this cannot be proven due to the lack of macroscopic findings. In the lower section of the core, MS starts to increase. Subsequently, MS values sharply decrease at the boundary of the next layer, and within the collapsed, infilled burial chamber, it drops to less than a tenth of its value in the layer between 357–312 cm.

In contrast, in the upper part of the previous layer and in the following layer, which can be distinguished macroscopically, MS values start to increase and fluctuate between 0.25 and 0.33, which can be considered significant for the entire section. At the boundary of the next layer, from 287 cm, MS values in the previous layer sharply decrease and maintain a fluctuating but constant value until the upper part of this layer (up to 242 cm). This suggests the formation of a homogenous soil layer with a thickness of about 40 cm, which was exposed to similar environmental impacts during its development. In the upper part of this layer, MS starts to increase again, and in the next thin layer (between 232–242 cm, construction break, former trampled surface) it shows high MS values ranging between 0.18–0.3.

In the next layer (between 232–162 cm), magnetic susceptibility sharply drops again compared to the prominent values of the underlying compacted surface, then slowly increases until the top of the layer, although this increase is not very significant (from 0.05 to 0.1).

The following layer can be distinctly separated from the layer below. MS values increase significantly at the boundary of the layer over a few centimeters, defining another distinguishable layer with a thickness of 10 cm between the depths of 162 and 152 cm. The average MS value here is 0.17. From 152 cm, MS values suddenly decrease to about a third of the upper part of the previous layer, and fluctuate between 0.05–0.1 in a relatively balanced manner. This pattern defines another layer between the depths of 152–97 cm.

Based on the changes in MS values, another layer can be distinguished between 97–62 cm. Here, MS increases compared to the previous layer. Significant changes within the layer itself cannot be distinguished; the values fluctuate between 0.13–0.24 in a balanced manner without a clear trend. Between 62 and 22 cm, another 40 cm thick layer can be separated. MS shows a sudden significant decrease (from 0.24 to 0.06) from the boundary of the previous layer, followed by slow but balanced growth until the top of the layer, where it reaches a value of 0.16.

Based on the changes in magnetic susceptibility in the uppermost layer, a distinct layer can be identified from the depth of 22 cm, where the relatively high MS values range between 0.27–0.37. According to macroscopic examinations, this layer corresponds to the A and B horizons of the recent soil. However, this is the only layer where

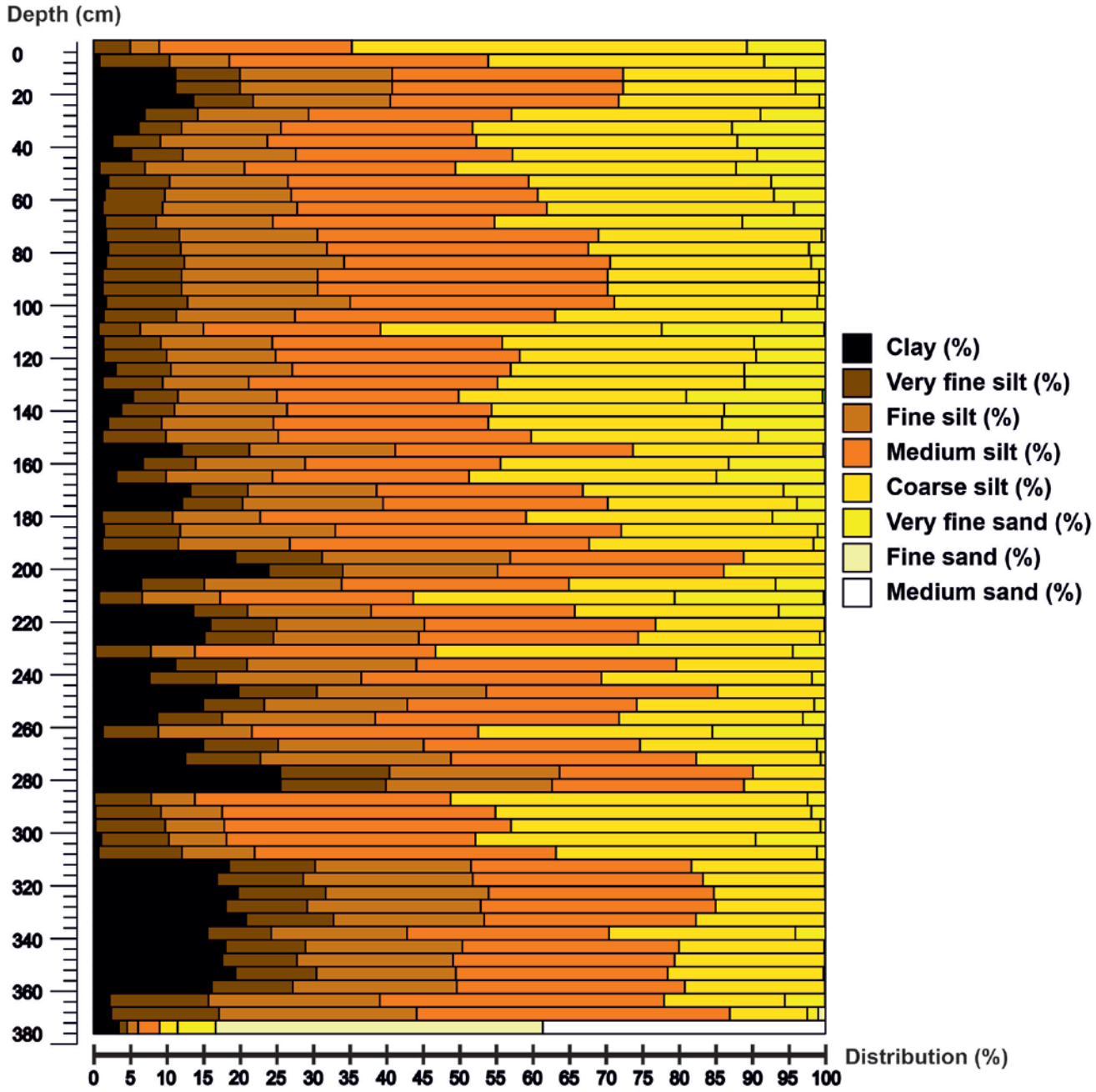

Fig. 4. The percentage distribution of the grain size composition in the stratigraphic sequence from the clay fraction to the medium sand fraction.

macroscopically distinguishable layers cannot be precisely determined based on the LS due to the transitional nature of the A and B horizons.

Sedimentological and Pedological Results

Based on the results of LOI measurements (organic matter, inorganic matter, and carbonate content) as well as the grain size composition, the drill core profile can be divided into layers that are very similar to the macroscopic observations of the kurgan. The measured values of the LOI measurements and the grain size composition can be observed (Figs 4 and 5).

In the lowest, well-defined section of the drilling core (between 377–357 cm), the organic matter content is very low (around 1%), and the carbonate content is less than 1%. In terms of grain size composition, this layer differs significantly from the construction layers of the kurgan itself. In the lowest sample of this layer, the fine sand fraction exceeds 40%, and very fine sand is around 5%. The clay fraction averages 6%, and the remaining ~50% of the particle size is composed of aleurite fractions. Upwards in this layer, the proportion of sand decreases significantly (Fig. 4).

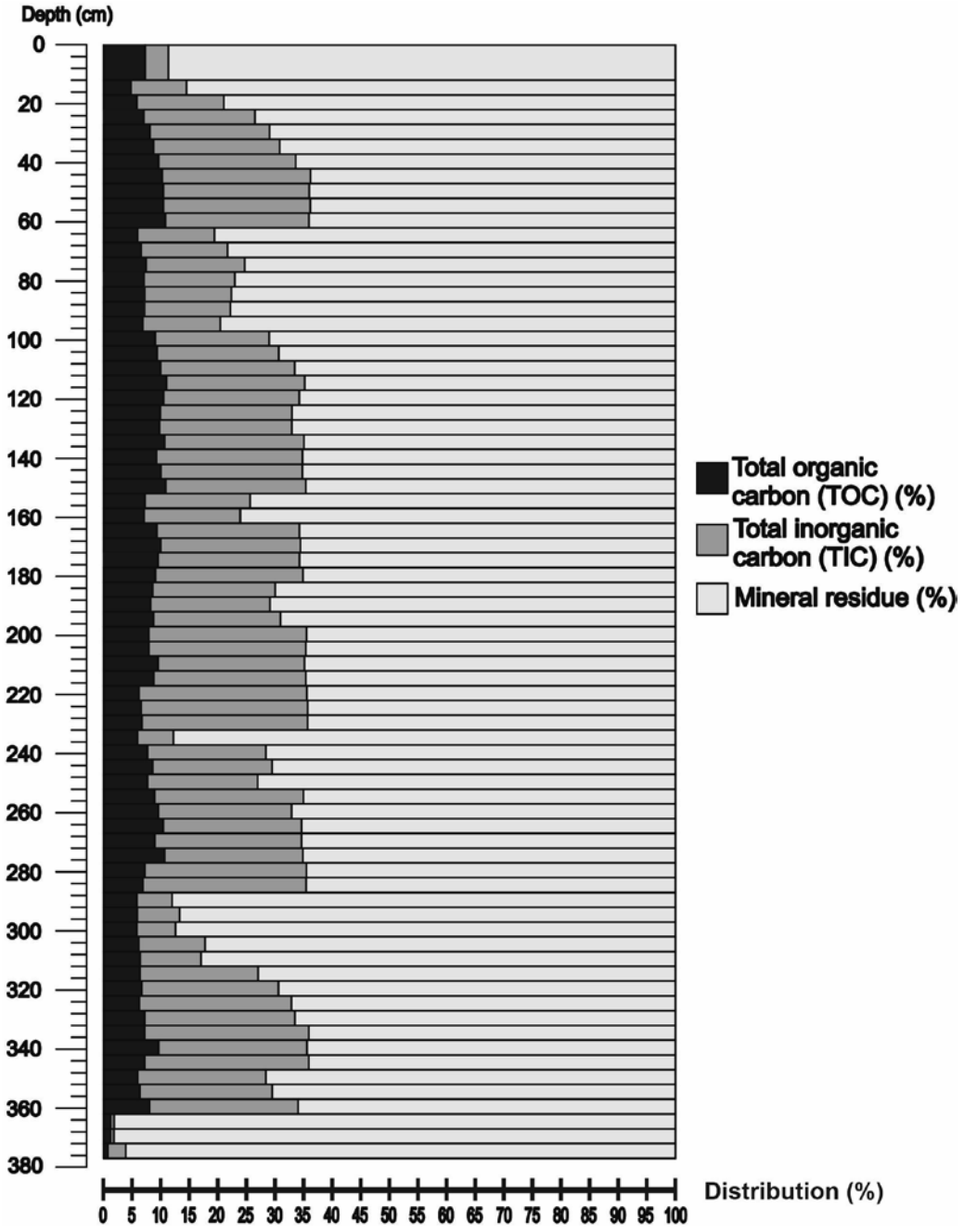

Fig. 5. The results of the Loss on Ignition (LOI) measurements conducted on samples extracted from the drill core of the mound—The organic matter content is represented by the Total Organic Carbon (TOC), while the other carbonate material is represented by the Total Inorganic Carbon (TIC).

The next layer (between 357–312 cm) is characterized by an average organic matter content of around 7% and increased carbonate content (average: 25%). Significant changes can also be observed in the grain size composition, with an average clay content of 18%, while the sand fractions practically disappear. Therefore, the sediment can be considered predominantly composed of aleurite, with the domination of finer aleurite fractions.

In the subsequent layer (between 312–287 cm), significant changes occur in the values of the carbonate content – it decreases to an average of 8.5%, about one-third of the previous layer. Very fine sand reappears in the grain size composition, and the aleurite fractions shift towards coarser aleurite, while the average clay content decreases to less than 1%.

The next well-defined layer is located between 287–232 cm. There are no significant changes in the organic matter content, but the carbonate content starts to increase abruptly at the boundary of the layer and remains constant throughout the entire layer (average: 22%). The clay content increases significantly, reaching the maximum value (25%) of the entire section. The proportion of the sand fractions

– except for a spike to 15% – is lower than 1%, and the proportion of finer and coarser aleurite fractions is more balanced.

Another layer can be distinguished between 232–152 cm. Both the organic matter content (average: 8.2%) and the carbonate content (average: 25%) show a slight increase, resulting in a decrease in inorganic matter. The clay content varies with a minimum of less than 1% and a maximum of 24%. This layer is also predominated by aleurite fractions, although in some samples, a higher percentage of very fine sand can be observed.

The layer between 152–97 cm does not show any changes in LOI results. What distinguishes this layer is a significant decrease in clay content to an average of 2%, and a shift in grain size composition towards coarser particles, with an average of about 10% for the very fine sand fraction.

Between 97 and 62 cm, there is a decrease in both organic matter and carbonate content, but no significant changes are observed in the grain size composition. The layer between 97 and 62 cm shows a decrease in organic matter and carbonate content, but there are no significant changes in the grain size composition.

Between 62 and 22 cm, both organic matter and carbonate content start to increase again, showing approximately constant values within the entire layer, with averages of around 9.5% and 24%, respectively. Changes in the grain size composition include an increase in clay fraction (average: 6%), which shows continuous growth within the layer, from 2% to 11%. The dominant particle fraction in this layer is still the medium and coarse aleurite.

The uppermost level of the drill core sequence is the recent surface soil (22 cm – surface), where both organic matter and carbonate content are lower than in the previous level. The carbonate content decreases from 15% to 4% towards the surface, while organic matter shows relatively constant values with an average of 6%. A noteworthy change is a decrease in the clay content from 11% to 0%, as well as a decrease in finer aleurite fractions, with the coarser aleurite and sand content exceeding 10% at the surface.

Chronological results

A radiocarbon dating was performed on a charred wood sample extracted from the 347–352 cm depth of the kurgan, specifically from the level of the collapsed burial chamber at the bottom of the kurgan. This measurement dates back the calendar age of the charcoal residue between 3352 and 3090 BC as it can be observed (Table 1).

Table 1. Results of radiocarbon measurements conducted on charcoal remains found in a sample taken from a depth of 347–352 cm in the borehole drilled into the Árpád Mound.

Lab Code	Material	Depth (cm)	14C yr BP	±	(cal AD/BC) (±2s)
DeA-23159	charcoal	347–352	4496	33	cal BC 3352–3090

DISCUSSION

Based on the analysis of samples extracted from a total of 377 cm of drilling and the measurements performed on them, the kurgan can be divided into a total of 12 different layers. These 12 layers, in terms of their origins, can be consolidated into four distinct construction phases. Among the measurement data, due to significant, temporally varying human disturbances, the grain composition in addition is only moderately useful, whereas the magnetic susceptibility results are highly effective for defining these layers. The results of the particle size distribution measurements, although they show some variability, do not exhibit any particular trend and generally present a fairly homogeneous picture, except for the presence of larger, sandier lenses derived from the bedrock. Therefore, in terms of particle size distribution, the entire profile—including the material of the kurgan—is quite homogeneous, consisting mostly of silt. This is evidence of a loess origin, upon which chernozem-like soil has developed, detectable on both the former and current surfaces. Only the lowermost sample of the profile deviates significantly from the relatively homogeneous composition.

The lowest level, beginning at 377 cm, has already penetrated the ancient Pleistocene sand, as indicated by the presence of sandy sediment. Additionally, human influence is evident, as the reddish color and prominent MS values suggest the use of ochre, which frequently appears earlier times, in Bronze Age cultures as well. Red-painted skulls are known, for instance, at Dévaványa (Ecsedy, 1979) and the Black Sea periphery of the East European Plain (Anthony, 2007). In the latter case, ochre-painted face masks were also created (Ślusarska, 2006). It can be assumed that it was present during the funeral ceremonies here as well, given that it appeared in these earlier and later periods.

The subsequent layers between 357–242 cm (Fig. 6) can also be interpreted as a collapsed burial chamber containing bone fragments and charred wooden remains. Precise identification of these remains requires further investigation; however, the age of the charcoal remnants indicates that the deposition and disturbance of the layer, thus the formation of the burial level, can be dated to cal BC 3352–3090. This timeframe, considering the geographical context, supports the kurgan's association with the Yamnaya culture. The soil material of the kurgan generally developed on loess bedrock, which overlaid the sandy deposits. This resulted in chernozem soil, indicative of the presence of grassy steppes during the Holocene. Between 232–243 cm, the first deposition level likely concluded, as evidenced by the high MS values indicating an ancient soil surface and the denser character of the layer, which suggests a former trampled surface (Sümegi *et al.*, 2015).

The subsequent layer, between 232–152 cm (Fig. 6), represents another thin stratum formed later than the previous one due to its stratigraphic position. This layer consists of disturbed soil material with low MS values and lacks any

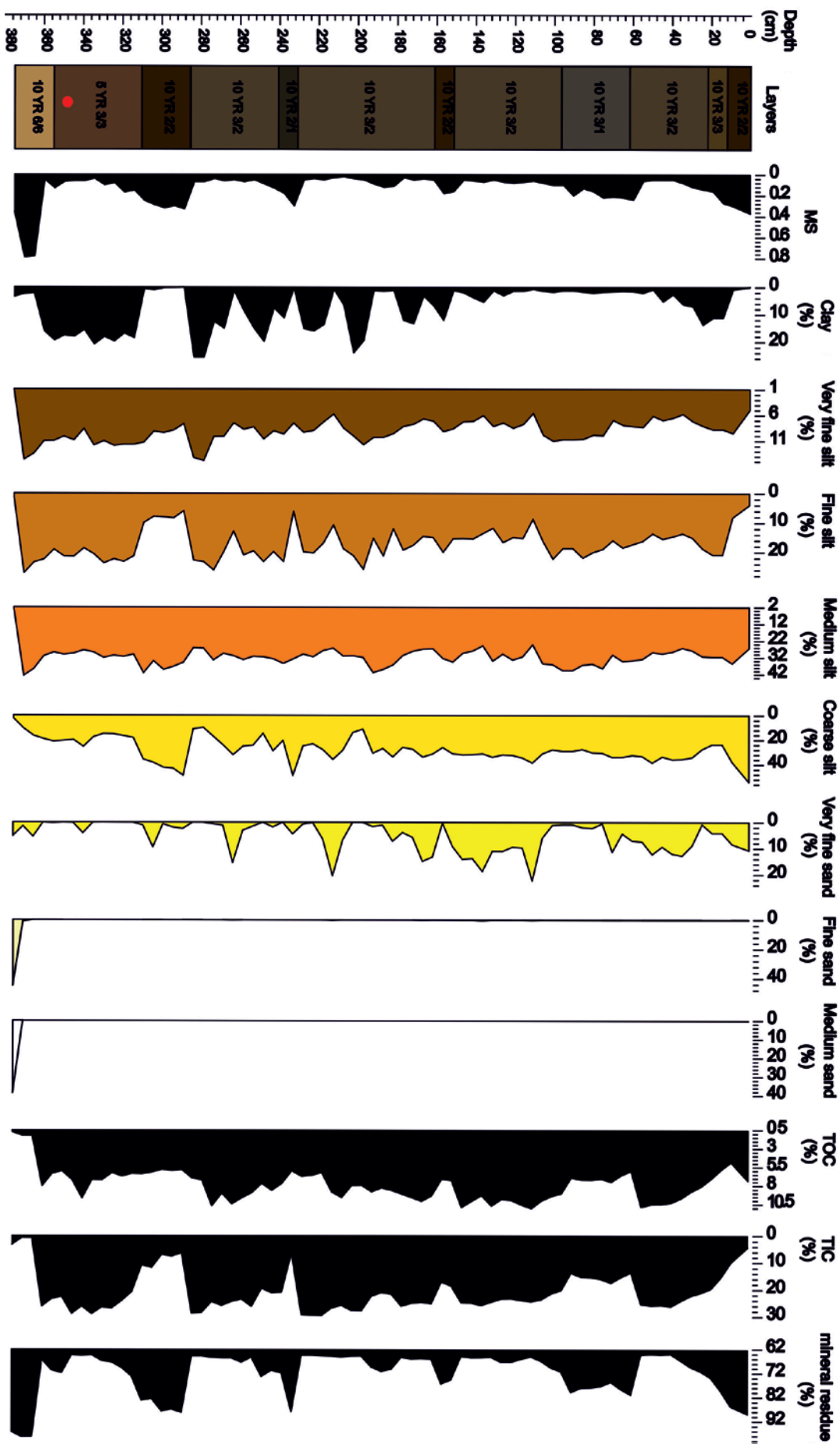

Fig. 6. The summarized results of the analyses conducted on samples extracted from the drilling profile of the mound, including magnetic susceptibility (MS) tests, grain size composition measurements, and the results of organic matter and carbonate content measurements (TOC, TIC). The red dot indicates the depth from which the sample, subjected to radiocarbon analysis, was taken.

indications of a burial chamber. It is followed by a denser layer, characterized by higher than decreasing MS values, representing an ancient trampled surface indicative of another pause in deposition (Sümegi *et al.*, 2015).

The third deposition layer, located between 152–62 cm, also consists of disturbed soil material. Based on the disturbance, it is presumably a former burial level or a level that indicates activity connecting to rituals or burial feasts, containing significant bone remains, snail shells, and black organic matter spots. This requires further examination to clarify the bone fragments found at the deposition level. This level is followed by the fourth deposition level, from 62 cm to the surface, which features a very thin, approximately 20 cm, undisturbed chernozem soil development at the top.

The upper two levels should be discussed together, considering that the level of the third deposition is surprisingly close to the surface. This proximity can be attributed to alterations made to the kurgan's surface in the late 1800s, due to the construction of a 12-meter-high obelisk at its center. This explains the appearance of the very thin and young undisturbed soil layer, as well as the close proximity of the former human-disturbed level to the surface. It is conceivable that the kurgan, in its original state, was higher, meaning this level might have been deeper beneath its surface. Additionally, future geochemical investigations would be necessary to determine how the limestone content of the obelisk on the kurgan's surface has influenced the mineral composition of the kurgan's soil, with particular attention to its carbonate content. In addition, further drilling will be necessary in the future around the mound to better distinguish the conditions influenced by natural and anthropogenic processes.

Beyond their intrinsic significance, the investigations conducted at the Árpád Mound have also provided an opportunity to contextualize the kurgan within a local framework, corroborating and complementing existing findings. Similar to other kurgans studied in this region of the Great Hungarian Plain (e.g., Császárné Mound – Cseh *et al.*, 2022, Vesszős Mound – Cseh *et al.*, 2019), the initial construction layer of the Árpád Mound dates back to the Late Copper Age – Early Bronze Age, corresponding to the primary expansion period of the Yamnaya culture in the Carpathian Basin. Each of these kurgans was constructed in multiple stages, with previous studies suggesting several burial phases. However, actual burial chamber materials have not yet been identified in other kurgans, which is now successfully done at the Árpád Mound. The appearance of sandy bedrock at a depth of 372 cm supports the hypothesis proposed by Sümegi *et al.* (2015) that kurgans were originally constructed on elevated surfaces to mitigate the effects of high groundwater levels near the Tisza River. This elevation created an artificial microenvironment where typical chernozem soil could develop instead of water-affected chernozem. Thus, it can be concluded that the Árpád Mound not only supports but also significantly supplements the findings of previous studies conducted on kurgans in this region.

CONCLUSIONS

The geoarchaeological investigation of the Árpád Mound has provided valuable insights into kurgan construction and the environmental conditions of the Great Hungarian Plain during the Late Copper to Early Bronze Age. Through soil and sediment analysis, magnetic susceptibility measurements, and radiocarbon dating, the study revealed a complex, multi-phase construction process involving ritualistic practices within the 4 distinguishable construction layers. Sedimentological data allowed for the reconstruction of Holocene environmental conditions and the development of Chernozem soils indicative of grassland vegetation. This highlights the dynamic landscape of the Carpathian Basin. The study also underscores the impact of prehistoric human activity on local soils, creating distinct anthropogenic layers. Radiocarbon dating aligns the mound's construction with the Yamnaya culture, emphasizing its cultural and territorial significance. In conclusion, this study enhances our understanding of kurgan construction, prehistoric environmental conditions, and the interplay between ancient societies and their environment, paving the way for future geoarchaeological research in the region.

REFERENCES

Alexandrovskiy, A.L., 1996. Natural Environment as Seen in Soil. Eurasian Soil Science 29, 245–254.

Alexandrovskiy, A.L., 2000. Holocene Development of Soils in Response to Environmental Changes: The Novosvobodnaya Archaeological Site, North Caucasus. Catena 41, 238–248.

Anthony, D.W., 2007. Horse, the Wheel and Language. How Bronze-Age riders from the Eurasian steppes shaped the Modern World. Princeton University Press, Oxford.

Barczi, A., 2004. The importance of pedological investigations in Holocene palaeoecological reconstructions. Antaeus 27, 129–134.

Barczi, A., Sümegi, P., Joó, K., 2003. Adatok a Hortobágy paleoökológiai rekonstrukciójához a Csípohalom talajtani és malakológiai vizsgálata alapján. Földtani Közlöny 133, 421–432.

Bede, Á., Salisbury, R.B., Csathó, A.I., Czukor, P., Páll, D.P., Szilágyi, G., Sümegi, P., 2015. Report of the complex geoarcheological survey at the Ecse-halom kurgan in Hortobágy, Hungary. Central European Geology 58, 268–289.

Bokhorst, M.P., Vandenberghe, J., Sümegi, P., Łanczont, M., Gerasimenko, N.P., Matviishina, Z.N., Markovic, S.B., Frechen, M., 2011. Atmospheric circulation patterns in central and eastern Europe during Weichselian Pleniglacial inferred from loess grain-size records. Quaternary International 234, 62–74.

Cseh, P., Sümegi, P., Törőcsik, T., Náfrádi, K., Kustár, R., Balázs, R., Szilágyi, G., 2019. Preliminary data of the geoarchaeological analyses on the Vesszős-halom (mound) at Pusztaszer. Archeometriai Műhely 1786-271X 16(3).

Cseh, P., Molnár, D., Makó, L., Sümegi, P., 2022. Geoarchaeological Analyses of a Late-Copper-Age Kurgan on the Great Hungarian Plain. Quaternary 5, 20.

Dani, J., Horváth, T., 2012. Őskori Kurgánok a Magyar Alföldön. A Gödörsíros (Jamnaja) Entitás Magyarországi Kutatása az Elmúlt 30 Év során. Áttekintés és Revízió; Archaeolingua Alapítvány: Budapest, Hungary, p. 215.

Dean, W.E., 1974. Determination of carbonate and organic matter in calcareous sediments and sedimentary rocks by loss on ignition;

comparison with other methods. Journal of Sedimentary Petrology 44, 242–248.

Dearing, J., 1999. Environmental Magnetic Susceptibility: Using the Bartington MS2 System; Chi Publishing: Keniloworth, UK, p. 43.

Demkin, V.A., Kashirskaya, N.N., Demkina, T.S., Khomutova, T.E., El'tsov, M.V., 2008. Paleosol studies of burial mounds in the Ilovlya River valley (the Privolzhskaya Upland). Eurasian Soil Science 41, 115–127.

Derese, C., Vandenberghe, D.A.G., van Gils, M., Vanmontfort, B., Meirsman, E., Mees, F., van den Haute, P., 2010. Establishing a chronology for landscape evolution around a final palaeolithic site at Arendonk-Korhaan (NE Belgium): First results from optically stimulated luminescence dating. Mediterranean Archaeology and Archaeometry 10, 43–51.

Ecsedy, I., 1979. The People of the Pit-Grave Kurgans in Eastern Hungary. Fontes Archaeologici Hungaricae; Akadémiai Kiadó: Budapest, Hungary, p. 147.

Google Earth, available online: https://earth.google.com/web/@46.55717139,19.96879911,88.25628787a,247.64467606d,35y,0h,4.43218031t,0r/data=OgMKATA (accessed on 20 July 2024).

Gyalog, L., Síkhegyi, F., 2005. Magyarország Földtani Térképe, M = 1:100,000; A Magyar Állami Földtani Intézet Kiadványa: Budapest, Hungary.

Hertelendi, E., Csongor, É., Záborszky, L., Molnár, I., Gál, I., Győrffy, M., Nagy, S., 1989. Counting system for high precision C-14 dating. Radiocarbon 32, 399–408.

Hieri, O., Lotter, A., Lemcke, G., 2001. Loss on Ignition as a Method for Estimating Organic and Carbonate Content in Sediments: Reproducibility and Comparability of Results. Journal of Paleolimnology 25, 101–110.

Holdridge, L.R., 1947. Determination of world plant formations from simple climatic data. Science 105, 367–368.

IUSS Working Group WRB. World Reference Base for Soil Resources 2014, Update 2015. International Soil Classification System for Naming Soils and Creating Legends for Soil Maps; World Soil Resources Reports No. 106; FAO: Rome, Italy.

Joó, K., Barczi, A., Sümegi, P., 2007. Study of soil scientific, layer scientific and palaeoecological relations of the Csípő-mound kurgan. Atti della Società Toscana di Scienze Naturali A112, 141–144.

Kinnaird, T.C., Dixon, J.E., Robertson, A.H.F., Peltenburg, E., Sanderson, D.C.W., 2013. Insight on topography development in the Vasilikós and Dhiarizos Valleys, Cyprus, from integrated OSL and landscape studies. Mediterranean Archaeology and Archaeometry 13, 49–62.

Lehmkuhl, F., Nett, J.J., Pötter, S., Schulte, P., Sprafke, T., Jary, Z., Antoine, P., Wacha, L., Wolf, D., Zerboni, A., Hošek, J., Markovi ć, S.B., Obreht, I., Sümegi, P., Veres, D., Zeeden, C., Boemke, B., Schaubert, V., Viehweger, J., Hambach, U., 2021. Loess landscapes of Europe – Mapping, geomorphology, and zonal differentiation. Earth Science Reviews 215, 103496. https://doi.org/10.1016/j.earscirev.2020.103496

Michéli, E., Csorba, A., Szegi, T., Dobos, E., Fuchs, M., 2019. The soil types of the modernized, diagnostic based Hungarian Soil Classification System and their correlation with the World reference base for soil resources. Hungarian Geographical Bulletin 68, 109–117.

Molnár, B., 2015. A Kiskunsági Nemzeti Park Földtana és Vízföldtana; JATE Press: Szeged, Hungary, p. 524 (in Hungarian).

Molnár, M., Janovics, R., Major, I., Orsovszki, J., Gönczi, R., Veres, M., Leonard, A.G., Castle, S.M., Lange, T.E., Wacker, L., 2013. Status report of the new AMS 14C sample preparation lab of the Hertelendi Laboratory of Environmental Studies (Debrecen, Hungary). Radiocarbon 55, 665–676.

Munsell, A.H., 2000. Munsell Soil Color Charts; Munsell Color Company: Baltimore, MD, USA, p. 29.

Pál, B.A.S., Katalin, J. 2003. Joó Adatok a Hortobágy paleoökológiai rekonstrukciójához a Csípő-halom talajtani és malakológiai vizsgálata alapján. Földtani Közlöny, 133, 421–432 (in Hungarian)

Péczely, G. 1979. Éghajlattan; Nemzeti Tankönyvkiadó: Budapest, Hungary, p. 342, (in Hungarian)

Pető, A., Barczi, A. (Eds), 2011. Kurgan Studies. An environmental and archaeological multy roxy study of burial mounds in the Eurasian steppe zone.. BAR International Series 2238, BAR Publishing, Oxford.

Reimer, P., Austin, W., Bard, E., Bayliss, A., Blackwell, P.G., Ramsey, C.B., Butzin, M., Cheng, H., Edwards, R.L., Friedrich, M., 2020. The IntCal20 Northern Hemisphere radiocarbon age calibration curve (0–55 cal kBP). Radiocarbon 62, 725–757.

Rómer, F., 1878. Compte-Rendu de la Huitième Session à Budepest 1876. I. Résultats Généreaux du Mouvement Archéologique en Hongrie; Magyar Nemzeti Múzeum: Budapest, Hungary, p. 187.

Ślusarska, K., 2006. Funeral rites of the Catacomb community: 2800–1900 BC. Ritual, thanatology and geographical origins. Baltic-Pontic Studies, 13.

Stefanovits, P., 1972. Talajtan. Mezőgazda Kiadó: Budapest, Hungary, p. 380.

Sümegi, P., 2002. A Negyedidőszak Földtanának és Őskörnyezettanának Alapjai; JATE Press: Szeged, Hungary, 262 p.

Sümegi, P., Persaits, G., Gulyás, S., 2012. Woodland-Grassland Ecotonal Shifts in Environmental Mosaics: Lessons Learnt from the Environmental History of the Carpathian Basin (Central Europe) during the Holocene and the Last Ice Age Based on Investigation of Paleobotanical and Mollusk Remains; Springer Press: New York, NY, USA, pp. 17–57.

Sümegi, P., Bede, Á., Szilágyi, G., 2015. Régészeti geológia, geoarcheológiai és környezettörténeti elemzések régészeti lelőhelyeken. A földtudományok és a régészet kapcsolata. Analyses of Archeological Geology, Geoarcheology and Environmental History on the Archeological Sites Contat between Earth Sciences and Archeology. Archeometriai Műhely 12, 135–150.

Sümegi, P., Molnár, D., Gulyás, S., Náfrádi, K., Sümegi, B.P., Törőcsik, T., Persaits, G., Molnár, M., Vandenberghe, J., Zhou, L., 2019. High-resolution proxy record of the environmental response to climatic variations during transition MIS3/MIS2 and MIS2 in Central Europe: The loess-paleosol sequence of Katymár brickyard (Hungary). Quaternary International 504, 40–55.

Wentworth, C.K., 1922. A Scale of grade and class terms for clastic sediments. Journal of Geology 30, 377–392.

Wikimedia Commons. Pannonian Basin Geographic Map Blank Cropped. Available online: https://upload.wikimedia.org/wikipedia/commons/2/27/Pannonian_Basin_geographic_map_blank_croped.svg (accessed on 10th June 2024).

Zaitseva, G.I., Chugunov, K.V., Bokovenko, N.A., Dergachev, V.I., Dirksen, V.G., 2005. Chronological study of archaeological sites and environmental change around 2600 BP in the Eurasian steppe belt (Uyuk Valley, Tuva Republic). Geochronometria 24, 97–107.

Zhen, Q., 2021. Exploring the Early Anthropocene: Implications from the long-term human-climate ineractions in Early China. Mediterranean Archaeology and Archaeometry 21, 133–148.